Proceedings of ICONE14
International Conference on Nuclear Engineering
July 17-20, Miami, Florida, USA

ICONE14-89221

LOCAL INTERFACIAL STRUCTURES IN HORIZONTAL BUBBLY FLOW WITH 90-DEGREE BEND

Seungjin Kim
Nuclear Engineering, 1870 Miner Circle
University of Missouri – Rolla,
Rolla, MO 65401

Gunol Kojasoy, Jung Han Park
Department of Mechanical Engineering
University of Wisconsin-Milwaukee,
Milwaukee, WI 53201

Joseph M. Kelly
US Nuclear Regulatory Commission
Mail Stop T10 K08
Washington, DC 20555

ABSTRACT

Present study investigates the geometric effects of flow obstruction on the distribution of local two-phase flow parameters and their transport characteristics in horizontal two-phase flow. The round glass tubes of 50.3mm in inner diameter are employed as test sections, along which a 90-degee elbow is located at L/D=206.6 from the two-phase mixture inlet. In total, 15 different flow conditions are examined within the air-water bubbly flow regime. The detailed local two-phase flow parameters are acquired by the double-sensor conductivity probe at four different axial locations. The effect of elbow is found to be evident in both the distribution of local parameters and their development. The elbow clearly promotes bubble interactions resulting in significant changes in interfacial area concentration. It is also found that the elbow-effect propagates to be more significant further downstream (L/D=250) than immediate downstream (L/D=225) of the elbow. Furthermore, it is shown that the elbow induces significant oscillations in the flow in both vertical and horizontal directions of the tube cross-section. Characteristic geometric effects due to the existence of elbow are also shown clearly on the axial development of one-dimensional interfacial area concentration and void fraction.

INTRODUCTION

The interfacial structure and its transport characteristics are directly related to the transfer of mass, momentum and energy of a two-phase flow system. The knowledge on local interfacial structures in horizontal two-phase flow is of particular importance, because the interfacial structures, regime transition and fluid particle interaction mechanisms differ significantly from those in the vertical flow, and little local database are available for horizontal two-phase flow configurations while many studies have been carried out for vertical configuration. Considering that the horizontal flow configurations are frequently encountered in both traditional light water reactor systems and advanced reactor systems, such as APWR, ABWR and ACR-700, lack of experimental database and accurate models present a serious shortcoming in thermal-hydraulic reactor system analysis. Furthermore, in many practical engineering systems including the nuclear

reactor, the coolant channels are interconnected via various flow obstructions, through which significant changes in interfacial structure and regime transition occur. As noted in some previous studies[1-3], it is clear that such flow obstructions further complicate the interfacial structures and hence interfacial transfer characteristics. However, no study has been done to address the geometric effects on the distribution of local two-phase flow parameters due to the existence of flow restrictions. Therefore, detailed studies on two-phase flow structures in horizontal two-phase flow with flow restriction can make a significant improvement in the current capability of thermal-hydraulic assessment of a nuclear reactor system.

Some the limited studies on local two-phase flow parameters in horizontal flow include the work done by Sharma et al.[4], Iskandrani and Kojasoy[5], and Lewis et al.[6] In their studies, internal structures and local two-phase flow parameters in various horizontal two-phase flow regimes were studied in detail. Franca and Lahey[7], on the other hand, performs one dimensional analysis of horizontal two-phase flow using the drift flux model, where they correlated the distribution parameter and drift velocity for plug, slug and separated horizontal two-phase flow configurations. Up to date, however, there has been no study on the development of local two-phase flow parameters under the influence of flow obstruction, and there is a significant lack of fundamental knowledge on its geometric effects. Furthermore, the detailed local studies are also essential in developing the interfacial area transport equation[8,9] and in the application of two-fluid model[10] for horizontal two-phase flow. In view of this, present study focuses on the effect of a 90-degree elbow on the development of local two-phase flow parameters and their transport characteristics in horizontal air-water bubbly flow via a round tube.

EXPERIMENTAL FACILITY

A simplified schematic diagram of the horizontal two-phase test facility employed in the present study is shown in Figure 1. The test section is made with round Pyrex tubes with inner diameter of 50.3 mm, along which a 90-degee Elbow is installed at L/D=206.6 from the two-phase mixing chamber. The Elbow has a radius of curvature of 76.2 mm with an $(L/D)_{elbow}$ of approximately 6. The detailed dimension of the elbow is shown in the inset of Figure 1. Along the test section, four local instrumentation ports are installed as denoted in the figure as P1 through P4. The local pressure tap located right after the two-phase mixing chamber is chosen as a reference point and denoted as P0 (or L/D=0). Hence, the first local measurement port, P1 is located at L/D=197 from P0 (or 9.5 diameters before the 90-degree Elbow), and the ports P2, P3 and P4 are located at L/D=225, 250 and 329 from P0 (or 18.1, 43.9 and 122.7 diameters downstream of the elbow), respectively.

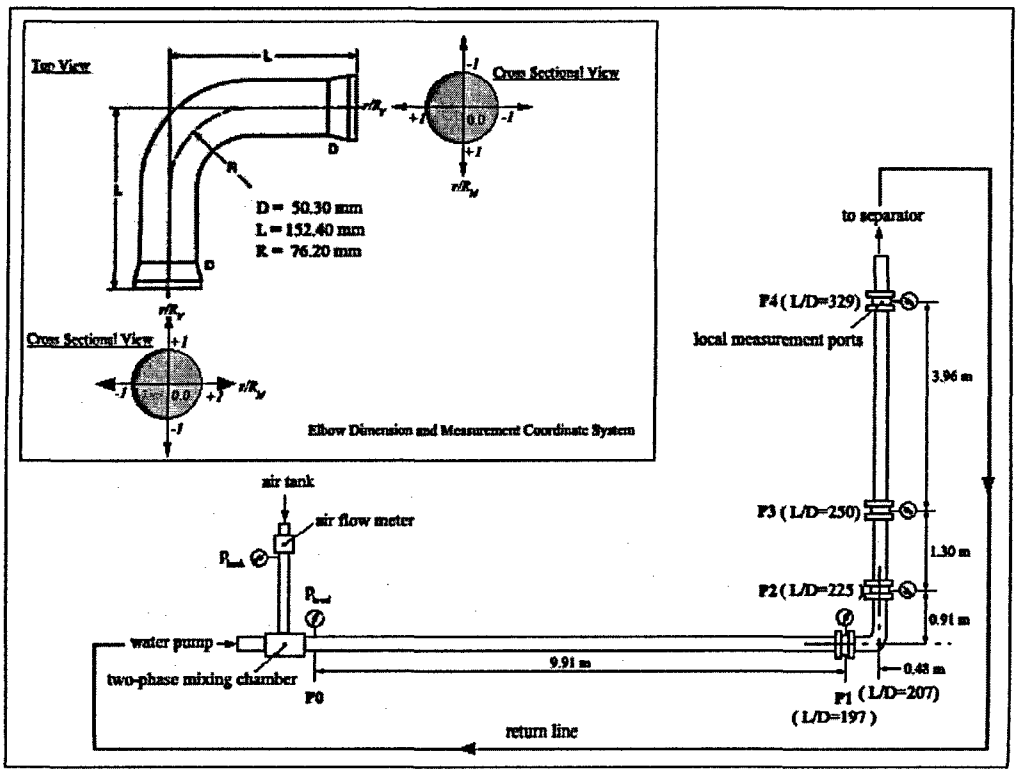

Figure 1. A simplified schematic diagram of the 50.3 mm ID horizontal two-phase flow test facility with 90-degree Elbow junction (shown in top view and not scaled).

The double-sensor local conductivity probe is employed in acquiring the local two-phase flow parameters. The local ports are designed such that the probe can be traversed and rotated in radial and azimuthal directions of the tube cross-section, respectively. The local two-phase flow parameters acquired by the double-sensor conductivity probe includes: bubble frequency (f_b), bubble velocity (u_g), void fraction (α) and interfacial area concentration (a_i).

Accounting for the asymmetric distribution of bubbles in the horizontal two-phase flow, the local measurements are made across the entire tube diameter. At ports P1 and P4, a local probe is traversed in vertical direction along the tube cross-section diameter (r/R_V), assuming that the flow is symmetric along the vertical line. It also assumes that the effect of elbow in interfacial structure is negligibly small at P1 and P4. At ports P2 and P3, on the other hand, the probe is traversed along both vertical and horizontal (r/R_H) directions along the tube cross-section diameters, considering that the elbow may significantly affects the interfacial structures. In view of identifying the inner and outer section of the elbow, $r/R=0$ is chosen to be at the center of tube cross-section, and the positive r/R denotes inner or upper half of horizontal and vertical tube diameters, respectively. Similarly, the negative r/R indicates the outer or lower half of horizontal and vertical tube diameters, respectively. The measurement coordinate system described here is shown in the inset of Figure 1. In total, measurements are made at 23 local points along each tube diameter.

EXPERIMENTAL RESULTS AND DISCUSSIONS

Test Conditions

In total, 15 different j_g & j_f combinations are investigated, all in bubbly two-phase flow conditions. The test conditions are labeled as Runs 1 through 15 and are summarized in Table 1. Since the local gas flow rate is a function of local pressure, gas flow rates shown in the Table are based on the standard atmospheric pressure condition.

In view of benchmarking the reliability of acquired local data, the local superficial gas velocity, $\langle j_{g,loc} \rangle$ at each measurement port is compared with that calculated based on the α and u_g acquired by the conductivity probe. They are relatively in good agreements within $\pm$ 10% difference as shown in Figure 2.

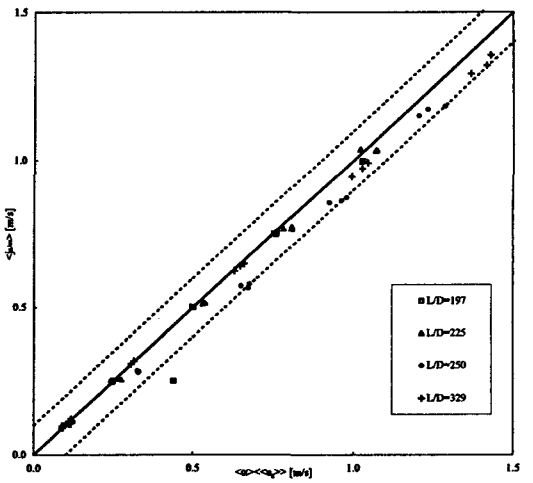

Figure 2. Comparison of the local superficial gas velocity, $\langle j_{g,loc} \rangle$ measured by flow meter with $\langle \alpha u_g \rangle$ acquired by the conductivity probe. ±10 % shown in dotted lines.

Local Interfacial Structures

In Figure 3(a) and (b), characteristic profiles of local α and a_i obtained in Run 5 ($j_{g,atm}$=0.320 m/s and j_f=4.047 m/s) are shown as an example. In the figures, profiles along the vertical and horizontal radii are shown for the parameters acquired at four different measurement ports. As noted earlier, the measurements are made only along the vertical radius, R_V at Ports 1 and 4 (or L/D=197 and 329), assuming that the flow is symmetric along the vertical axis of cross-section. At Ports 2 and 3, on the other hand, profiles along the horizontal radius, R_H are also acquired.

Table 1. Test conditions

	Run 1	Run 2	Run 3	Run 4	Run 5
$j_{g,atm}$ [m/s]*	0.116	0.124	0.127	0.312	0.320
j_f [m/s]	3.762	4.051	4.335	3.765	4.047
	Run 6	Run 7	Run 8	Run 9	Run 10
$j_{g,atm}$ [m/s]*	0.329	0.644	0.659	0.673	0.985
j_f [m/s]	4.338	3.772	4.048	4.338	3.764
	Run 11	Run 12	Run 13	Run 14	Run 15
$j_{g,atm}$ [m/s]*	1.004	1.031	1.336	1.372	1.406
j_f [m/s]	4.049	4.313	3.760	4.051	4.332

*$j_{g,atm}$ is the superficial gas velocity equivalent to the standard atmospheric pressure condition.

As shown in the figures, α and a_i profiles show similar trend. It is interesting, however, that both α and a_i along the horizontal direction are distributed such that bubbles reside in the outer-half of the tube cross-section ($R_H < 0$) right after the elbow (L/D=225), then they migrate toward the inner-half ($R_H > 0$) further downstream (L/D=250). This suggests that the elbow induces severe flow oscillation in horizontal directions of the tube cross-section. In Run 5, the flow oscillation phenomenon can be found in both vertical and horizontal directions across the tube cross-section. In fact, it is found in all of the flow conditions examined in the present study that such oscillation is a characteristic elbow effect. The degree of oscillation varies depending on the flow conditions as will be shown later.

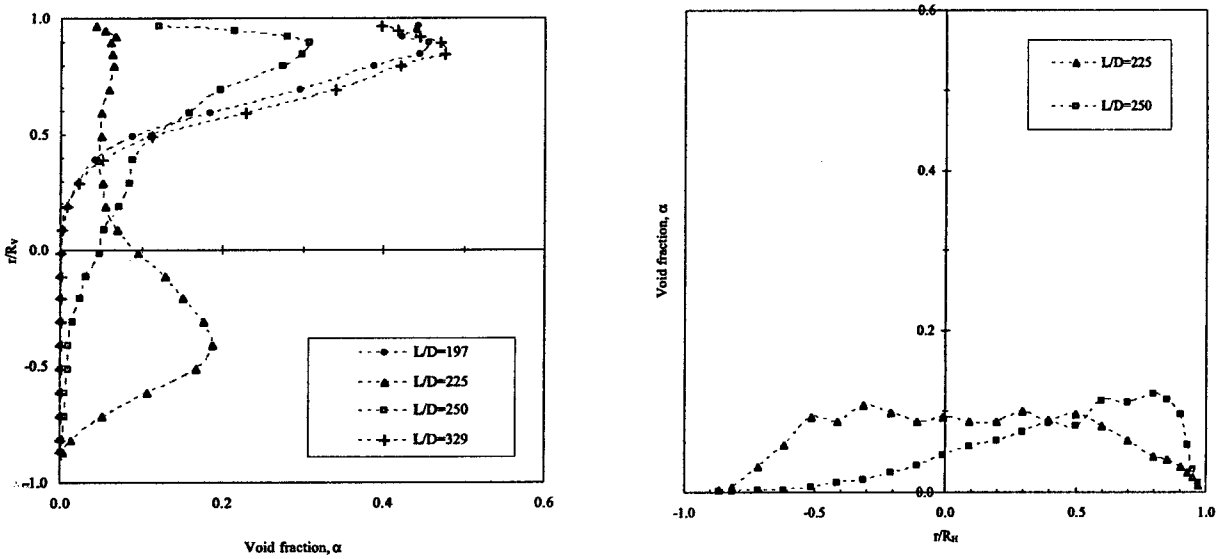

(a) Profiles of void fraction, α

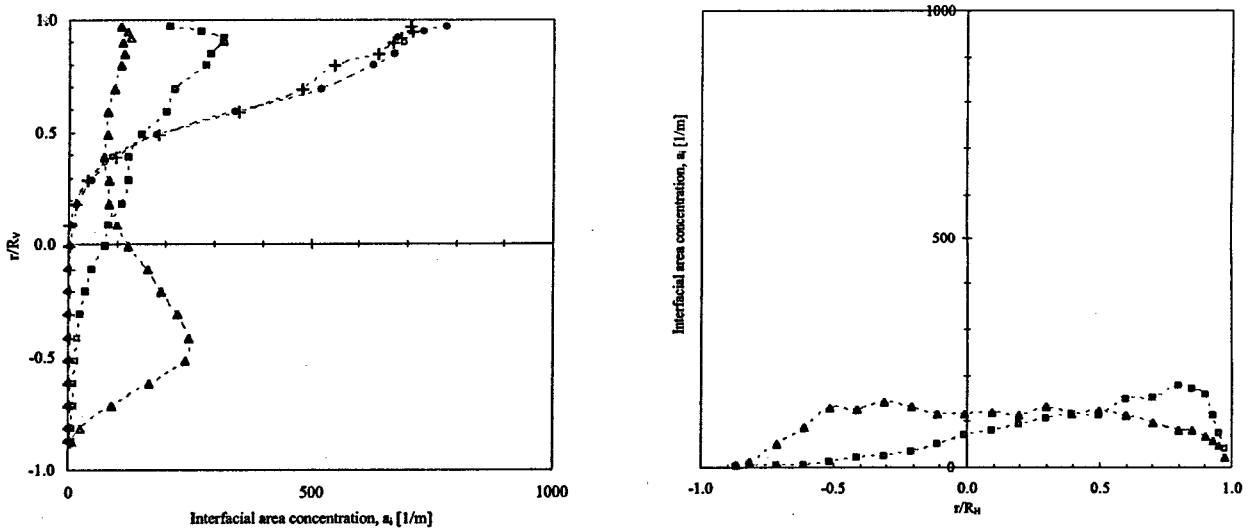

(b) Profiles of interfacial area concentration, a_i

Figure 3. Profiles of local two-phase flow parameters in Run 5 at different L/D's along the vertical and horizontal radii.

In view of examining the effects of gas and liquid flow rates in the development of local two-phase flow parameters, the profiles of α and a_i along the vertical radius of the tube cross-section, R_V are plotted for different flow conditions in figures 4 and 5. In Figure 4, the superficial gas flow rates, j_g are varied to 0.127, 0.673 and 1.406 m/s while the superficial liquid flow rate, j_f is fixed at 4.3 m/s (Runs 3, 9 and 15). In Figure 5, on the other hand, j_f's are varied to 3.765, 4.047 and 4.338 m/s while j_g is fixed at 0.3 m/s (Runs 4, 5 and 6). In general, it is found that the profiles of α resemble to those of

a_i, which is characteristic of the bubbly flow regime. The locations of local peak and the degree of peaking depend on both gas and liquid flow rates. In all of the test conditions, both α and a_i tend to peak near $r/R_V \approx +0.5$. However, the distribution pattern changes right after the elbow (L/D=225), which indicates that the elbow has significant effects in flow structure. After examining figures 4 and 5, following characteristics can be found in the flow structures along the vertical tube radius, R_V:

At L/D=197 (or 9.5 diameters before the elbow): In all flow conditions, bubbles reside mostly upper half of the tube, resulting in local peaks of α and a_i near the top of the tube cross-section ($0.75 < r/R_V < 1$). Bubble distribution tends to spread more along R_V with increasing gas flow rates.

At L/D=225 (or 18.1 diameters downstream of the elbow): The distribution of bubbles and location of local peaks of α and a_i depend primarily on the gas flow rates. In lower gas flow rates up to j_g=0.329m/s (Runs 1 through 6), bubbles migrate toward the lower half of the tube radius regardless the liquid flow rates. Hence, both α and a_i peak near the center of lower half of tube cross-section (i.e. $r/R_v \approx -0.5$), and the peaking phenomenon is more pronounced with increasing gas and liquid flow rates. When the gas flow rate is increased to j_g=0.7 m/s (Runs 7 through 9), bubbles migrate toward the center of tube cross-section, and α and a_i peak near r/R_v=0. As the gas flow rates increase further up to j_g=1.4 m/s (Runs 10 through 15), bubbles migrate further into the upper half of the cross-section, and both α and a_i peak near the center of upper half of tube cross-section (i.e. $r/R_v \approx +0.5$). It was found in all flow conditions that the degree of peaking depends primarily on the gas flow rates, such that local peaks of α and a_i become more pronounced with increasing gas flow rates.

At L/D=250 (or 43.9 diameters downstream of the elbow): In this region, bubbles redistribute themselves to recover their distribution pattern before the elbow. As will be shown later from the local profiles along the horizontal radius, R_H, however, significant elbow effect still remains and it is characterized by flow oscillations along the horizontal direction. Both α and a_i display single peak in the upper half of the tube cross-section ($r/R_V > +0.5$). The degree of peaking depends on both liquid and gas flow rates, such that the local peaking phenomenon becomes more pronounced with increasing liquid flow rates, whereas it damps out with increasing gas flow rates. In conditions with lower gas flow rates (Runs 1 through 3), the local profiles of α and a_i are almost fully recovered to those before the elbow, whereas the flow structures are yet to be recovered and bubbles are more distributed when $j_g > 0.3$ m/s,.

At L/D=329 (or 122.7 diameters downstream of the elbow): In this region, the flow structures are fully recovered in Runs 1 through 5 and 7 ($j_g < 0.3$ m/s, except for Run7). In Runs 6 and 8 through 15 ($j_g > 0.6$ m/s, except for Run 6), on the other hand, the flow structures are yet to be recovered. The characteristic features in the local two-phase flow parameters in this region are similar to those at L/D=250.

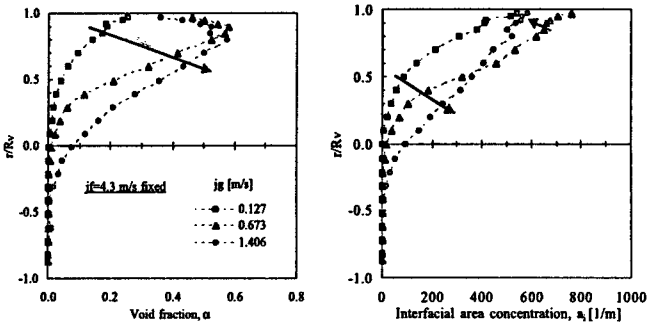

(a) L/D=197

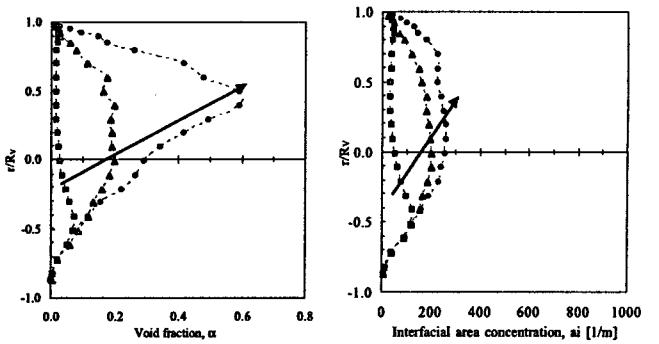

(b) L/D=225

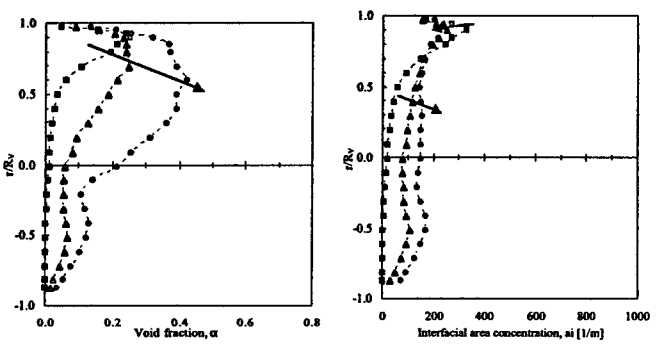

(c) L/D=250

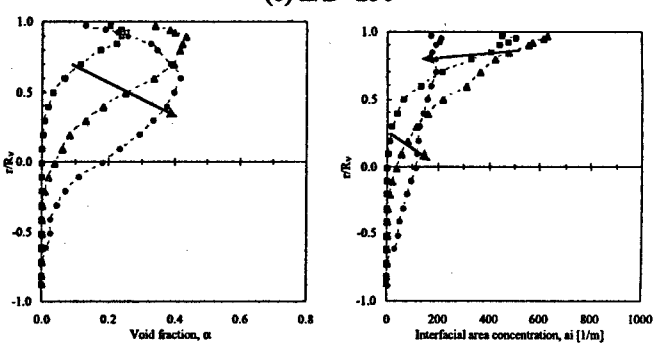

(d) L/D=329

Figure 4. Effect of gas flow rates on the flow structure along the vertical radius, R_V at different L/D's. j_f=4.3 m/s fixed & j_g=varied (Runs 3, 9 & 15). Arrows in the figure denote the direction of increasing gas flow rates.

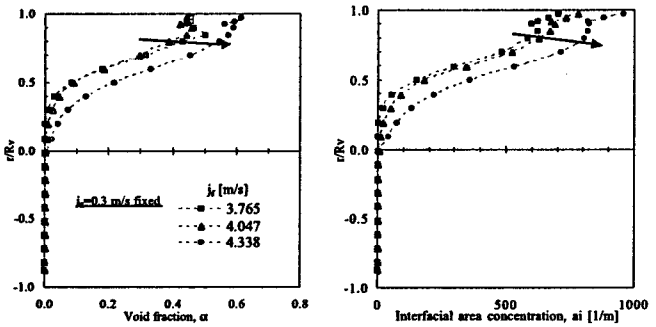

(a) L/D=197

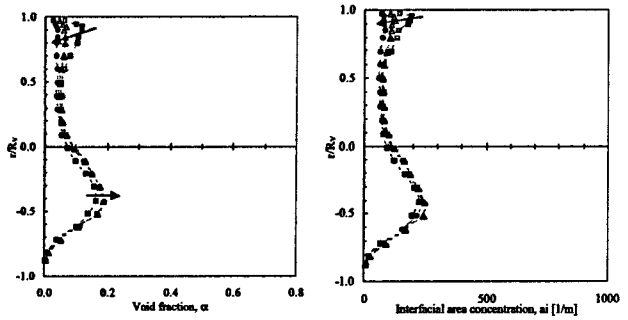

(b) L/D=225

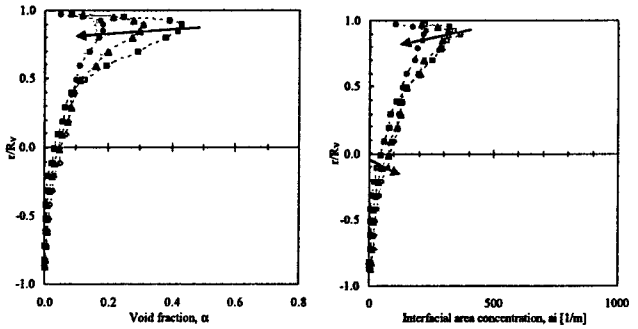

(c) L/D=250

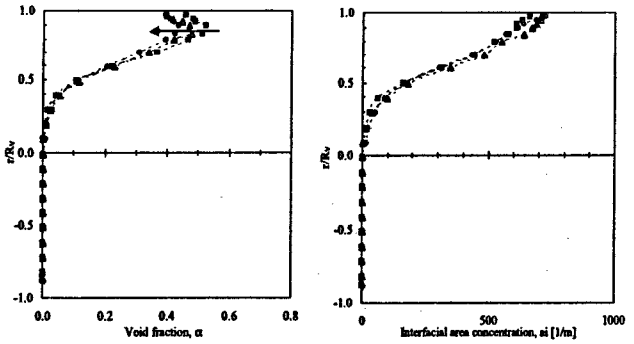

(d) L/D=329

Figure 5. Effect of liquid flow rates on the flow structure along the vertical radius, R_V at different L/D's. j_g=0.3 m/s fixed & j_f=varied (Runs 4, 5 and 6). Arrows in the figure denote the direction of increasing gas flow rates.

The effects of gas and liquid flow rates on the flow structures along the horizontal tube radius, R_H are examined in figures 6(a) and 6(b), respectively. As mentioned earlier, the local measurements along R_H are performed only at L/D=225 and 250, where the elbow effects can be most significant. Following characteristics can be found in the flow structures along the horizontal tube radius, R_H:

At L/D=225 (or 18.1 diameters downstream of the elbow): As shown in Figure 5(a), bubbles reside toward the inner radius of the tube cross-section (i.e, $R_H > 0$) when $j_g \approx 0.1$ m/s (Runs 1 through 3), but migrate toward the outer radius ($R_H < 0$) as the gas flow rates increase. Hence, when j_g is increased to 0.3 m/s (Runs 4 through 6), both α and a_i are distributed uniformly across R_H. Then, they peak near the outer side of the tube cross-section at $r/R_H \approx -0.5$, as the liquid flow rates increase further to $j_g > 0.6$ m/s (Runs 7 through 15). In this region, the liquid flow rates show similar effect as the gas flow rates, such that the peak locations change from the inner radius ($R_H > 0$) to the outer radius ($R_H < 0$) as the liquid flow rates increase. This is shown in Figure 5(b).

At L/D=250 (or 43.9 diameters downstream of the elbow): In this region, bubbles migrate toward the inner radius of the tube cross-section regardless the gas or liquid flow rates. Hence, both α and a_i peak near $r/R_H \approx +0.75$. The peaking phenomenon becomes more pronounced for both α and a_i with increasing gas and liquid flow rates as shown in figures 5(a) and 5(b), respectively.

ONE-DIMENSIONAL AXIAL DEVELOPMENT OF INTERFACIAL AREA AND VOID FRACTION

In view of one-dimensional transport of a_i and α, results obtained in two characteristic flow conditions, Runs 4 and 14 are plotted in figures 6(a) and 6(b), respectively. Here, the local parameters are averaged over the tube cross-section. It can be seen in Figure 6(a) that in Run 4, $<\alpha>$ increases while $<a_i>$ decreases as the flow passes across the Elbow (i.e. 197 < L/D < 250). Further downstream of the Elbow (250 < L/D < 329), however, an opposite trend is observed in $<a_i>$, such that it increases notably (~30%) with a small increase (~7%) in $<\alpha>$. This implies that in Run 4, the elbow promotes coalescence process, then the disintegration dominates as flow develops further downstream of the elbow.

In Run 14, on the other hand, $<\alpha>$ increases while $<a_i>$ decreases, regardless the elbow, along the axial direction of the flow. This implies that the coalescence process dominates throughout the test section in this condition. Considering that the liquid flow rates in both Runs are high ($j_f > 3.7$ m/s), and the gas flow rate in Run 14 ($j_{g,atm}$=1.372 m/s) is more than four times higher than that of Run 4 ($j_{g,atm}$=0.312 m/s), it is speculated that the high gas flow rate in Run 14 makes the coalescence mechanisms more dominant than the disintegration mechanisms. In Run 4, on the other hand, while the existence of elbow evidently promotes bubbles to coalescence, the high liquid flow rate and hence high turbulence makes disintegration mechanism dominate as the elbow effect starts to diminish further downstream of the elbow.

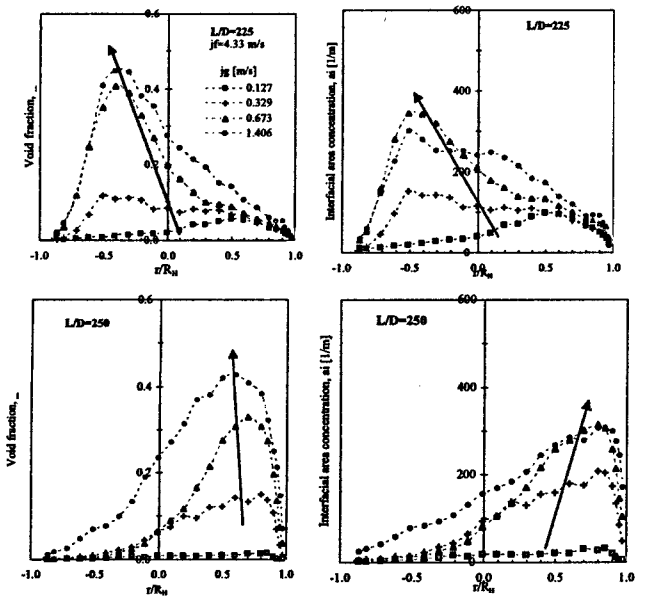

(a) Effects of gas flow rates (Runs 3, 9 and 15)

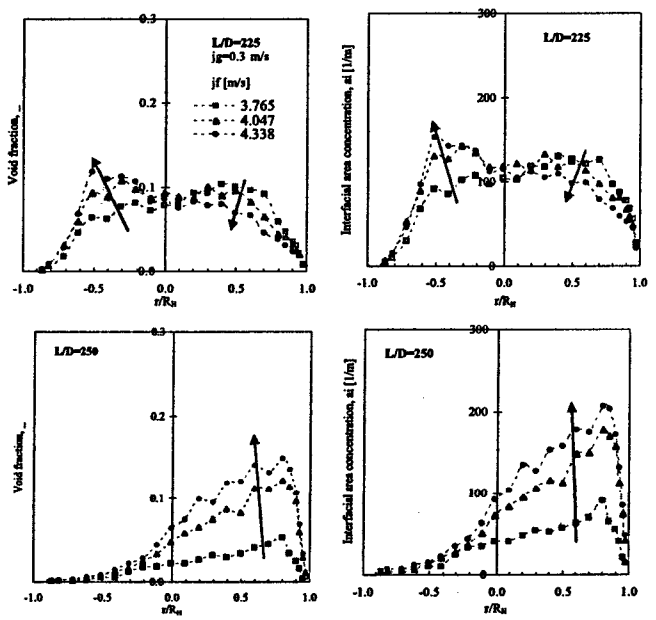

(b) Effects of liquid flow rates (Runs 4, 5 and 6)

Figure 5. Effect of gas and liquid flow rates on the flow structures along the horizontal radius, R_H at different L/D's. Arrows in the figure denote the direction of increasing flow rates.

In general, both $<a_i>$ and $<\alpha>$ increase with increasing gas flow for a given liquid flow rate. The effect of elbow, located between L/D=197 and 225, is more evident in the change of $<a_i>$. It is highlighted by a significant change of $<a_i>$ in that region. However, it is interesting to note that the change in $<\alpha>$ in this region is not as dramatic as $<a_i>$. In fact, in most flow conditions (except for Runs 13 and 6), the change in $<\alpha>$ in this region is minimal or less than 10%, while $<a_i>$ changes as much as 50%. This clearly indicates the elbow promotes various bubble interactions and result in either coalescence or disintegration. Furthermore, it is also interesting to note in many flow conditions that drastic changes in both $<a_i>$ and $<\alpha>$ do not appear right across the elbow in between L/D=197 and 225, but they do in between L/D=225 and 250. This indicates that the effects of elbow propagate further downstream and affect the development of interfacial structures.

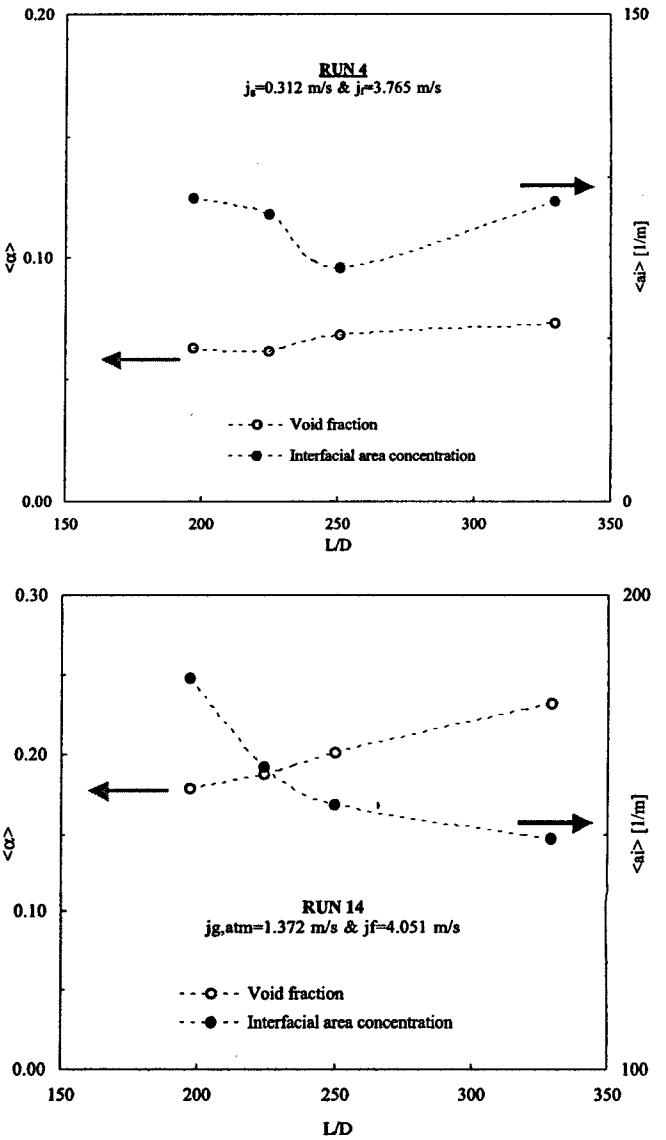

Figure 8. Axial developments of one-dimensional void fraction and interfacial area concentration in two characteristic flow conditions. (a) Run 4: $j_{g,atm}$=0.312 m/s & j_f=3.765 m/s (b) Run 14: $j_{g,atm}$=1.372 m/s and j_f=4.051 m/s

SUMMARY

Effects of a flow restriction on the development of two-phase flow structures and their transport characteristics are studied in horizontal two-phase flow configuration. A glass

tube of 50.3mm in inner diameter are employed as test sections, along which a 90-degee elbow is located at L/D=206.6 from the two-phase mixture inlet. In total, 15 different flow conditions are examined within the air-water bubbly flow regime.

The effect of a 90-degree elbow is found to be evident in configuring the flow structures. The elbow makes a significant effect on the local peaking phenomena in two-phase flow parameters, characteristic of a horizontal two-phase flow. It is also shown that the degree of peaking depends on both liquid and gas flow rates. Characteristic oscillations in the flow are induced by the elbow and are present in both vertical and horizontal directions across the channel cross-section. It is seen from the data that the effect of elbow propagates further downstream and is often more significant further downstream (L/D=43.9 after the elbow) than immediate downstream of the bend (L/D=18.1 after the elbow). The elbow clearly promotes bubble interactions resulting in significant changes in interfacial area concentration. Characteristic geometric effects of the bend are also shown clearly on the axial development of one-dimensional interfacial area concentration and void fraction.

ACKNOWLEDGEMENT

This work was supported by US Nuclear Regulatory Commission, Office of Nuclear Regulatory Research.

REFERENCES

1. M. Salcudean, D. C. Groeneveld and L. Leung, Effect of flow obstruction geometry on pressure drop in horizontal air-water flow, *Int. J. Multiphase Flow*, Vol. 9, No. 1, pp. 73-85, 1983
2. M. E. Salcudean and L. K. H. Leung, Two-phase pressure drop through obstructions, *Nucl. Eng. Des.*, Vol. 105, pp. 349-361, 1988
3. C. Wang, I. Y. Chen, Y. Yang and R. Hu, Influence of horizontal return bend on the two-phase flow pattern in small diameter tubes, *Experimental Thermal and Fluid Sci.*, Vol 28, pp. 145-152, 2004
4. S. Sharma, S. Lewis and G. Kojasoy, Local studies in horizontal gas-liquid slug flow, *Nucl. Eng. Des.*, 184, pp. 305-318 (1998)
5. A. Iskandrani and G. Kojasoy, Local void fraction and velocity field description in horizontal bubbly flow, *Nucl. Eng. Des.*, 204, pp. 117-128 (2001)
6. S. Lewis, W. L. Fu, and G. Kojasoy, Internal flow structure description of slug flow-pattern in horizontal pipe, Int. *J. Heat Mass Transfer*, 45, pp. 3879-3910 (2002)
7. F. Franca and R. T. Lahey Jr., The use of drift-flux techniques for the analysis of horizontal two-phase flows, Int. J. Multiphase Flow, Vol. 18, No. 6, pp. 787-801 (1992)
8. G. Kocamustafaogullari and M. Ishii, Foundation of the interfacial area transport equation and its closure relation, *Int. J. Heat and Mass Transfer*, 38, No. 3, p. 481 (1995)
9. M. Ishii and S. Kim, Development of one-group and two-group interfacial area transport equation, *Nucl. Sci. Eng*, Vol. 146, No. 3, pp257-273 (2004)
10. M. Ishii, *Thermo-fluid dynamic theory of two-phase flow*, Eyrolles, Paris (1975)